Proceeding of the IEEE
International Conference on Robotics and Biomimetics
Dali, China, December 2019

Variable Admittance Control for Human-Robot Collaboration in Robot-Assisted Orthopedic Surgery*

Jiawei Liang[12], Yuanyuan Yang[1], Yu Wang*[12], Shoubin Liu*[2], Mu Lu[12], Shiqi Song[12], Peng Zhang[1]
1 CAS Key Laboratory of Human-Machine Intelligence-Synergy Systems,
Shenzhen Institutes of Advanced Technology, Chinese Academy of Sciences
Email:{ jw.liang, yy.yang1, yu.wang, mu.lu, sq.song, zhangpeng}@siat.ac.cn
2 Harbin Institute of Technology, Shenzhen
Email:mesbliu@hit.edu.cn
**Corresponding authors are Yu Wang and Shoubin Liu.*

***Abstract* – In recent days, orthopedic surgical robots play an increasingly important role in surgeries. Impedance/admittance control is a commonly used method for orthopedic surgical robots. In this paper, we proposed a variable admittance control method for orthopedic surgery. Instead of modifying virtual damping or mass which present in previous variable admittance control works, we present a new method by setting a dynamic reference point for virtual spring to improve operators' boundary control ability during robot assisted orthopedic surgery. The reference point is the mean point of robot end effector trajectory in the past *T* period. The performance of the proposed controller was tested by conducting a cooperative experience, where all subjects were asked to finish a reaching task by using a Mini-robot.**

Index Terms - Variable Admittance Control, Orthopedic Surgery, Human-robot cooperation.

I. Introduction

With the development of robotics, human-robot collaboration has been increasingly used in industrial and medical filed. The orthopedic surgery is in great demand. Till now, orthopedic robots have been used in articular surgery[1], spine surgery[2], orthopedic trauma surgery[3], et.al. In the United States, there are approximately 600,000 total knee arthroplasties and 45,000 single-chamber knee replacement surgery each year[4]. And these numbers are also growing rapidly[5].

The physical properties of bone make robotics easier to apply in orthopedic surgery. At present, the US Food and Drug Administration (FDA) has authorized orthopedic surgical robots such as TSolution One, Sculptor RGA, Mako RIO, Mazor Renaissance, OMNIBotics, and ROSA for clinical application and commercialization. Orthopedic robots have become the most FDA-approved medical robot category. In orthopedic surgery, registration[6,7], navigation and Physical Human-Robot Interaction (pHRI) are all current research hotspots. Meanwhile, the pHRI is one of a key problem in robot-assisted orthopedic surgery.

Admittance/impedance control is a commonly used control scheme in pHRI [8]. The difference between admittance and impedance control is that the former calculates position from external force and fed to motion controller of the robot; on the opposite, the latter calculates force from the position. Admittance/impedance control is the same in the interactive method but admittance control is more popular because the lower position controller is easy to get [4].

Pure admittance control is not good enough. Researchers hope to make pHRI more comfortable and more effective through adjusting the admittance control parameters [9]. In previous works, many variable admittance control methods were developed to improve the maneuverability of robots. In [10], a variable admittance method was proposed for adjusting the virtual damping and virtual mass based on the inference of human intentions using desired velocity and acceleration. the proposed method was tested in a trajectory tracking task. Hsieh-Yu Li et.al [11] developed a variable admittance method for the micro-suturing task by directly mapping external force to virtual damping. In [12], a variable admittance method was proposed by using a multilayer feedforward neural network. The Cartesian velocity of the robot and the applied force by the operator as its inputs to modify online the virtual damping of the admittance. The neural network is trained online based on the error between the velocity of the minimum jerk trajectory model. The minimum jerk trajectory model was also used in [13-15]. Stavros et.al adjust virtual damping based on muscle co-contraction of the operator's arm by means of surface electromyography [16]. The proposed method was tested in a trajectory tracking task. The results indicate that proposed variable admittance method is better in required effort and accuracy.

All the previous works in variable admittance control manage to balance accuracy and flexibility through adjusting virtual damping or virtual mass. In this paper, a different variable admittance control method was proposed for orthopedic surgery. Neither virtual mass nor virtual damping would be changed, instead, a dynamic reference point was designed to improve the operator's boundary control ability.

* This research is supported by the National Natural Science Foundation of China (No. U1713218 and No. U1813213), and the Key Fundamental Research Program of Shenzhen (No. JCYJ20160608153218487 and JCYJ20180507182215361).

978-1-7281-6321-5/19//$31.00 ©2019 IEEE

The reference point and robot end effector were connected by virtual spring. The performance of the proposed controller was tested by conducting a cooperative experience where all subjects were asked to finish a reaching task by using a Mini-robot.

This paper is structured as follows. The background of orthopedic surgery is addressed in Section II. The proposed variable admittance method and the stability proof are discussed in Section III. An experiment is conducted in Section IV. Finally, the conclusion is presented in Section V.

II. Robot Assisted Orthopedic Surgery

Different ways of pHRI were developed in robot- assisted orthopedic surgery [17]. In this paper, we focus on Semi-active HRI, which is also called “hands on” human-robot collaboration. Take the total knee arthroplasty (TKA) surgery robot as an example (Fig. 1), the human can freely move robot within a certain area to remove diseased bone tissue (by cutting or grinding), and robot limits its end effector always in that area by using virtual fixtures. The precise positioning of the robot helps the operator get a better grinding surface to place the prosthesis [18]. The quality of the grinding boundary is critical to reducing surgical complications [19].

Compared with other fields of HRI, orthopedic surgery interaction has the following characteristics.

- Small work area;
- The grinding boundary is of great importance.

Since there are no completely rigid virtual fixtures, it is meaningful to improve the operator’s ability to control the grinding boundary.

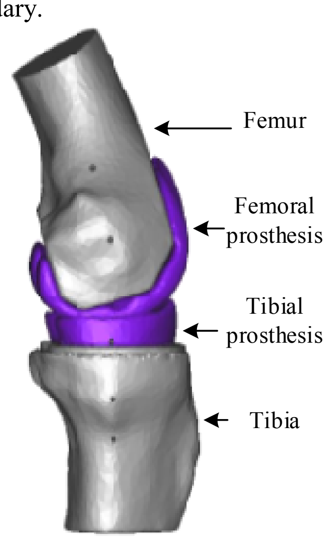

Fig. 1. TKA prosthesis

III. Method

The core idea of admittance control is to connect the external force and robot motion of the robot with a mass damping spring model. The original formula for admittance control is expressed as below [20].

$$F = \mathbf{M}\left(\ddot{X} - \ddot{X}_{\mathrm{d}}\right) + \mathbf{D}\left(\dot{X} - \dot{X}_{\mathrm{d}}\right) + \mathbf{K}\left(X - X_{\mathrm{d}}\right) \tag{1}$$

where X is end effector position in cartesian space, X_d represents the desired movement trajectory of the end-effector. F is the force applied by operator. **M**, **D** and **K** are virtual mass, damping and stiffness respectively. In “hands on” human-robot collaboration, since operator can freely move the robot, **K** and X_{d} is not needed. The admittance equation is like

$$F = \mathbf{M}\ddot{X} + \mathbf{D}\dot{X} \tag{2}$$

In previous works, variable admittance control is achieved by adjusting **M** and **D**. Considering the two characteristics of orthopedic surgery mentioned in Chapter II, we proposed the following variable admittance control method.

$$F(t) = \mathbf{M}\ddot{X}(t) + \mathbf{D}\dot{X}(t) + k\left(X(t) - X_r(t)\right) \tag{3}$$

Where

$$X_{\mathrm{r}}(t) = \frac{1}{T}\int_{t-T}^{t} X(t)dt \tag{4}$$

Fig. 2 shows how proposed method works. X is the current position of end effector, the red curve is the trajectory in the past T period, and k is virtual spring. The mean point in the past T period is used as a dynamic reference point X_{r}.

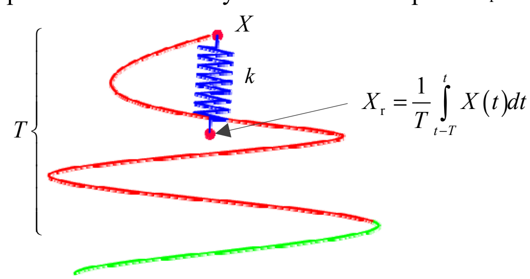

Fig. 2. The proposed variable admittance method. The mean point in the past T period is used as a dynamic reference point X_{r}.

In orthopedic surgery, when X moves back and forth rapidly in a small region (normally the surgical region is within 5 cm), by choosing a suitable T, X_{r} will stay in the regional center of the current operation. Therefore, the virtual spring k provides a soft constraint to the operator. The one-dimensional simulation of (3) shows in Fig. 3 (m=2kg, d=60Ns/m, k=60N/m). When X moves in one direction, the reference point X_{r} legs behind X. Once the external force equals zero, X moves backward and coincides with X_{r}. such characteristics make the robot easier to move the robot back when the end effector meets the boundary.

Mean reference point X_{r} makes the motion in orthopedic surgery more conservative, and safer.

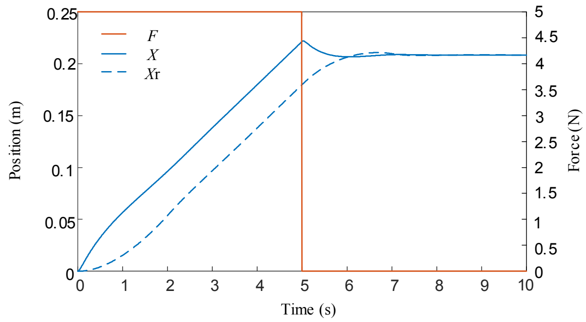

Fig. 3. The one-dimensional simulation of proposed method. When the external force F suddenly disappears, the robot will move backwards for a short distance under the action of the reference point X_r and the virtual spring k.

The whole control scheme is illustrated in Fig. 4. The cartesian velocity is calculated by proposed variable admittance controller, and followed by lower motion controller of the robot.

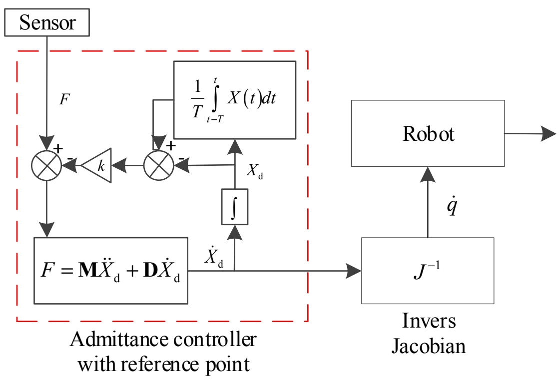

Fig. 4. Block diagram of proposed control method

The stability of proposed method is proved below. Assume that the tracking error of lower motion controller is zero which has unlimited bandwidth. In a single dimension, the system equation is

$$f(t) = m\ddot{x}(t) + d\dot{x}(t) + k\left[x(t) - \frac{1}{T}\int_{t-T}^{t} x(t)dt\right] \tag{5}$$

State equations are written below.

$$\begin{cases} \dot{X} = \mathbf{A}X + \mathbf{A}_1 X(t-\mathrm{T}) + \mathrm{B}u(x) \\ Y = \mathrm{C}X \end{cases} \tag{6}$$

where

$$\mathbf{A} = \begin{bmatrix} 0 & 1 & 0 \\ 0 & 0 & 1 \\ k/(mT) & -k/m & -d/m \end{bmatrix} \quad \mathbf{A}_1 = \begin{bmatrix} 0 & 0 & 0 \\ 0 & 0 & 0 \\ -k/m & 0 & 0 \end{bmatrix}$$

$$\mathrm{B} = \begin{bmatrix} 0 & 0 & 1/m \end{bmatrix}^{\mathrm{T}} \qquad \mathrm{C} = \begin{bmatrix} 0 & 1 & 0 \end{bmatrix}$$

The Laplace Transform of characteristic equation is

$$\begin{aligned} L\left(s, e^{-sT}\right) &= \det\left[s\mathbf{I} - \mathbf{A} - \mathbf{A}_1 e^{-sT}\right] \\ &= s^3 + \frac{d}{m}s^2 + \frac{k}{m}s + \frac{k}{mT}e^{-sT} - \frac{k}{mT} \end{aligned} \tag{7}$$

Since e^{-sT} have no roots in the complex plane and $mT > 0$, multiply mTe^{sT} at both sides of (7), then we get

$$\begin{aligned} h\left(s, e^{s}\right) &= mTe^{sT}L\left(s, e^{-sT}\right) \\ &= mTe^{sT}s^3 + dTs^2 + kTs - ke^{sT} + k \end{aligned} \tag{8}$$

Where $h\left(s, e^{s}\right)$ is called quasi-polynomial, and it has same roots with (7). By substituting $s = \mathrm{j}\omega$ into (8), we get

$$\begin{aligned} h(\omega) &= mTe^{\mathrm{j}\omega T}L\left(\mathrm{j}\omega, e^{-\mathrm{j}\omega T}\right) \\ &= mTe^{\mathrm{j}\omega T}(\mathrm{j}\omega)^3 + dT(\mathrm{j}\omega)^2 + kT\mathrm{j}\omega - ke^{\mathrm{j}\omega T} + k \end{aligned} \tag{9}$$

Separating the (9), real part $h_r(\omega)$ and imaginary part $h_i(\omega)$ can be get,

$$\begin{aligned} h_r(\omega) = {} & mT\omega^3\sin(\omega T) - dT\omega^2\cos(\omega T) - kT\omega\sin(\omega T) \\ & - k\cos(\omega T) + k \end{aligned} \tag{10}$$

$$\begin{aligned} h_j(\omega) = {} & -mT\omega^3\cos(\omega T) - dT\omega^2\sin(\omega T) + kT\omega\cos(\omega T) \\ & - k\sin(\omega T) \end{aligned} \tag{11}$$

According to [21], when (10) and (11) meet the following three conditions, quasi-polynomial (8) has only one eigenvalue lies in origin, and all other eigenvalues are in the left half plane.

1) $h_j(0) = h_r(0) = 0$

2) $h_r(\omega)$ and $h_j(\omega)$ have only simple real roots and these roots interlace.

3) For some $\omega_0 \in R$, $h_j'(\omega_0)h_r(\omega_0) - h_j(\omega_0)h_r'(\omega_0) > 0$

Apparently, condition (1) is fulfilled by substituting $\omega = 0$ into (10) and (11).

For proving condition (2), equation (10) and (11) is deformed to

$$h_r(\omega) = A\sin(\omega T + \alpha_1) + k \tag{12}$$

$$h_j(\omega) = A\sin(\omega T + \alpha_2) \tag{13}$$

where

$$A = \sqrt{\left(dT\omega^2 + k\right)^2 + \left(kT\omega - mT\omega^3\right)^2} \tag{14}$$

$$\alpha_1 = \arctan 2\left(\frac{-dT\omega^2 - k}{mT\omega^3 - kT\omega}\right) \tag{15}$$

$$\alpha_2 = \arctan 2\left(\frac{kT\omega - mT\omega^3}{-dT\omega^2 - k}\right) \tag{16}$$

By observing (15) and (16) we can get

$$\alpha_2 = \alpha_1 + \frac{\pi}{2} \tag{17}$$

Since m d k T are a positive constant number, then $A > k > 0$, substituting (17) into (13)

$$h_j(\omega) = A\cos(\omega T + \alpha_1) \tag{18}$$

When ω is not equal to 0, following (19) and (20) have same roots with (10) and (11).

$$\sin(\omega T + \alpha_1) = -\frac{k}{A} \tag{19}$$

$$\cos(\omega T + \alpha_1) = 0 \tag{20}$$

where $0 > -\frac{k}{A} \geq -1$.

Therefore, for any positive *m, d, k, T*, equation (19) and (20) have only simple real roots and these roots interlace. Fig. 5 shows how these roots are distributed.

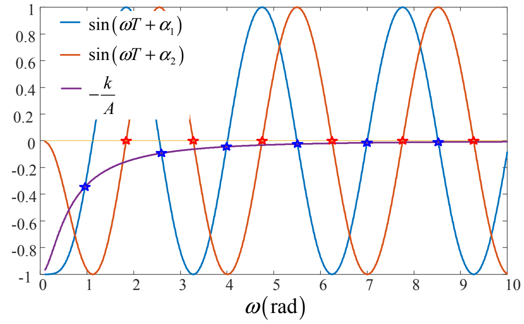

Figure 5. Roots of (19)(20)

For the condition (3), when $\omega \to \infty$,

$$h_r(\omega) \approx \hat{h}_r(\omega) = mT\omega^3 \sin(\omega T) \tag{21}$$

$$h_r(\omega) \approx \hat{h}_r(\omega) = -\mathrm{m}T\omega^3 \cos(\omega T) \tag{22}$$

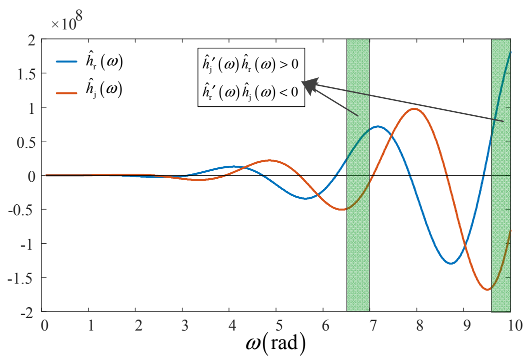

Fig. 6. When $\omega \to \infty$ the condition (3) is satisfied

As shown in Fig. 6, when ωT satisfies

$$2k\pi > \omega T > \pi/2 + 2k\pi \qquad k \in N \tag{23}$$

$\hat{h}_r(\omega)$ and $\hat{h}_r(\omega)$

$$\hat{h}_j'(\omega)\hat{h}_r(\omega) > 0 \tag{24}$$

$$\hat{h}_j'(\omega)\hat{h}_r(\omega) > 0 \tag{25}$$

then

$$\hat{h}_j'(\omega_0)\hat{h}_r(\omega_0) - \hat{h}_j(\omega_0)\hat{h}_r'(\omega_0) > 0 \tag{26}$$

Therefore condition (3) is satisfied when $\omega \to \infty$.

IV. Experimental Work

The purpose of this experiment is to prove that the operator's ability to control the boundary can be improved by proposed variable admittance control method. A Mini-robot with a force/torque sensor attached at the end-effector is used for experimental set-up, as shown in Fig.7.

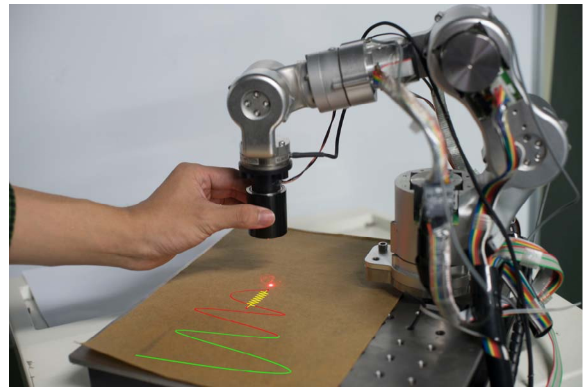

Fig. 7. A six DOF mini-robot. A laser pointer is attached to the end of the robot.

Mini-robot is a six DOF robot, its DH parameters is listed in Table 1 (the "*i*" in last column represents transmission ratio of corresponding joint).

The human operators can only freely move the robot in XY direction. A laser pointer is used to indicate current position. In collaboration mode, the external force is measured by F/T sensor and is input to the variable admittance controller (Fig. 4). The output velocity $\dot{V}$ is translated into joint velocities $\dot{q}$ and followed by lower motion controller.

It should be noted here that the stability proof proposed in Section III is based on a assume that the lower motion controller is perfect and yield no errors. But in practical experiment, unlimited bandwidth is impossible. Too small parameters will lead to an unstable collaboration. The lowest value of the virtual damping is found experimentally. And the parameters in this experiment is within the stable range. The robot is programmed to stop moving when the current position near a singular pose.

TABLE I
DH Parameters of Mini-robot

Link	*a*	*alpha*	*d*	*i*
1	a_1=70	90	d_1=110	100
2	a_2=85	0	0	100
3	0	-90	0	100
4	0	90	d_3=171	100
5	0	-90	0	100
6	0	0	60	100

As shown in Fig. 8, in this experiment, subjects were asked to move the robot from the start point to the endpoints along the dotted line. When the laser pointer just reached the boundary of A/B, subjects should immediately turn to the opposite direction. This task is designed to simulate the grinding operation in orthopedic surgery. The Square area A and B is forbidden area, and the dotted line represent the grinding trajectory. Different from real orthopedic surgery, there are no virtual fixtures in this experiment. The trajectory of end-effector will be recorded during the experiments.

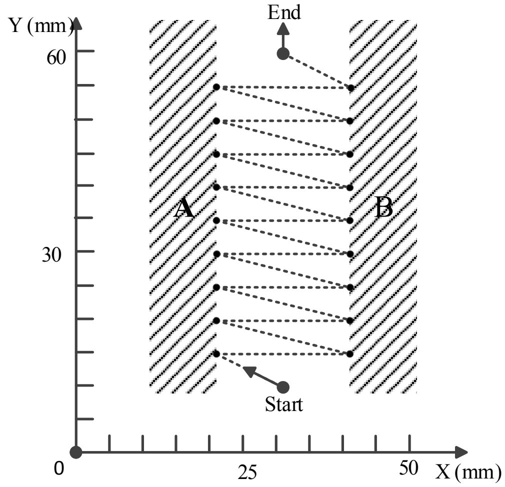

Fig. 8. Collaboration task in experiment. Subjects are required to move the robot from the starting point to the end point along the dotted line and not to exceed the boundary of A and B area.

Fig. 9 shows a recorded trajectory. During the collaboration task, the mean reference point (green) always stays in the central position of the trajectory in the past T period, which offered a soft constraint force to make operators easier to change direction while reaching the boundary of A/B. Once the end-effector(red) stop moving, the mean reference point will coincide with end-effector after T period.

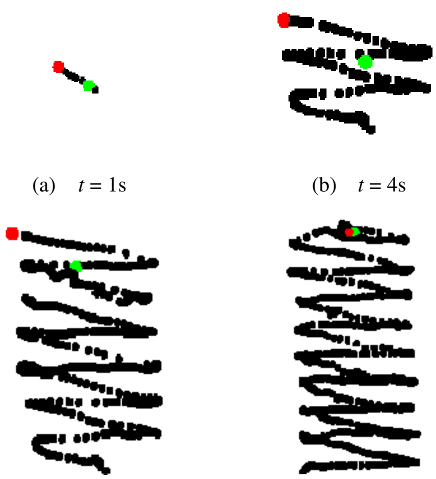

(a) t = 1s (b) t = 4s (c) t = 13s (d) t=16s

Fig. 9. One of the collaboration trajectories in the experiment. The red dot represents the current position X and the green dot represents the dynamic mean point X_r.

Fig. 10 shows the difference between the trajectory with/without mean reference point. Obviously, Fig. 10 (a) represents that when k=60N/m operators get a better ability in boundary control. Here the value of k is a value estimated based on the stiffness of the human arm.

The coordinates of the endpoints (red cross in Fig. 10) were collected to evaluate the quality of trajectories. Take the points on the left side as an example, ideally, these points should be in a straight line. Therefore, in Fig. 11, a least squares fit was conducted on these points on the left. The goodness of boundary control ability can be quantified by following equation.

$$\mathrm{RMSE} = \sqrt{\frac{1}{n}\sum_{i=1}^{n}\left(y_i - \hat{y}_i\right)^2} \tag{27}$$

where $\hat{y}_i$ are corresponding points on the fitted straight line. The smaller RMSE means a better boundary control ability.

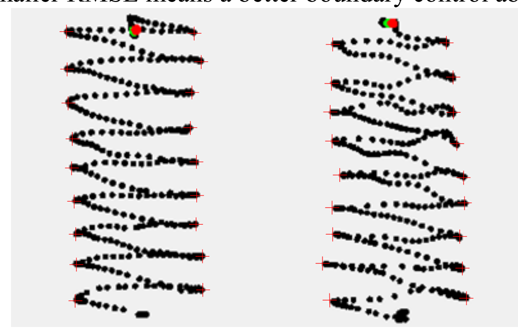

(a) k = 60 N/m (b) k = 0

Fig. 10. Comparison of trajectories with different k. When k=0 Virtual spring does not work, it means that the controller degenerates into a normal admittance controller.

Fig. 11 shows the RMSE of left points in Fig. 10. In this case, the RMSE is 0.625 in k = 60, and 0.898 in k = 0.

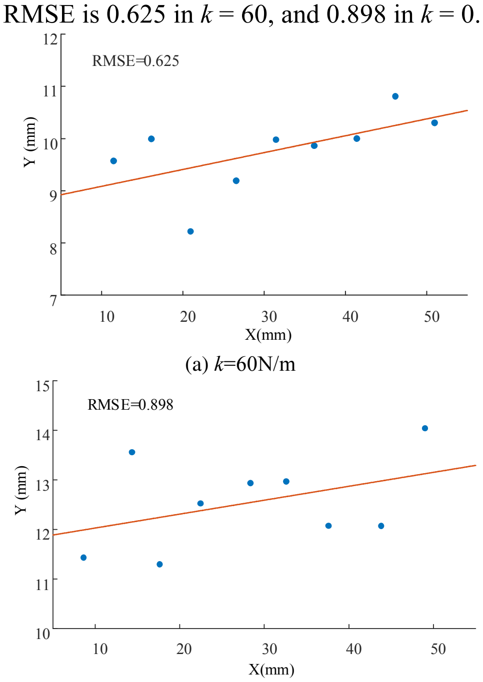

(a) k=60N/m

(b) k = 0

Fig. 11. Comparison of RMSE in different k. The smaller the value of RMSE, the better the boundary control ability.

There is a total of ten subjects in this experiment, one female, and one of the nine males is left handed. All of them have never worked with a robot before. Each of them is asked to complete the above task ten times. The parameters in this experiment are m = 2 kg, d = 40 Ns/m, T = 2 s and k = 60 N/m for the first five operations, k=0 for the last five times. All the endpoints are counted in the experiment. Since there are two sets of endpoints (left and right) in one recorded trajectory, and ten times a collaboration task for each subject, so, twenty RMSE results were collected for a single subject.

Fig. 12(a) shows the comparison of mean RMSE between k=60N/m, and k=0. All ten subjects have a lower mean RMSE while k=60N/m, which means the proposed variable admittance method does improve operator's boundary control ability. Subject 09 has a most obvious improvement for the mean RMSE has dropped by 38%, on the contrary, the mean RMSE of subject 03 has dropped by 10%. The mean RMSE of all ten subjects was reduced by 20%.

The difference between maximum and minimum RMSE is illustrated in Fig. 12(b). The smaller range of RMSE means better stability in human-robot collaboration. Except subject 06 and 10, all the other subjects have got a smaller range of RMSE by using the proposed method.

In Fig. 12(c), the box plot shows how the RMSE is distributed. It should be noted that the subjects were asked to finish the collaboration task between 15-20 seconds. And the task with k=60N/m was conducted before k=0. Compared with k=0, nine of all the ten subjects hold the opinion that they feel "easier and more comfortable" in the experiment with k=60N/m, except subject 05.

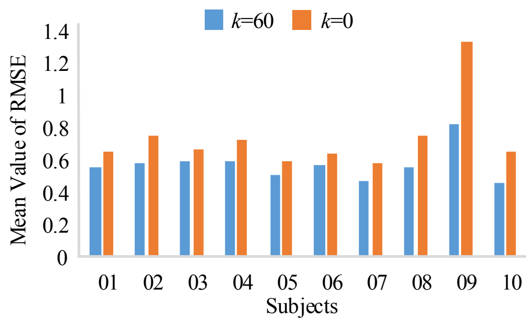

(a) Mean value of RMSE

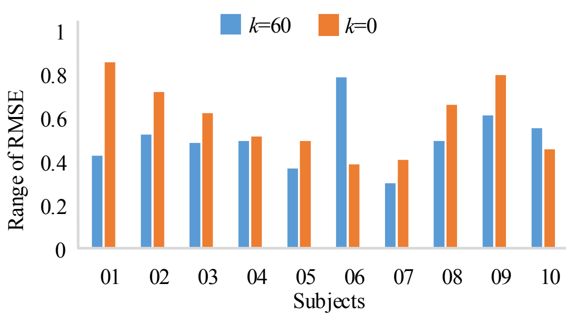

(b) Range of RMSE

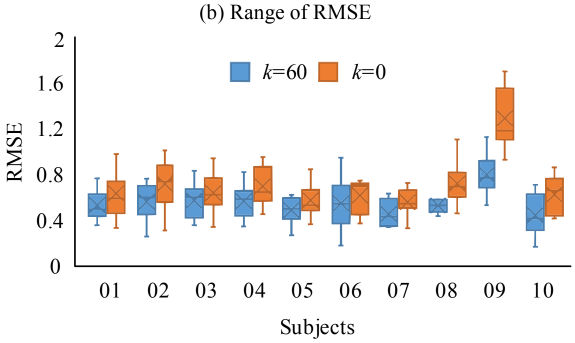

(c) RMSE

Fig. 12. RMSE of all ten subjects. Each subject performed the reaching task ten times. When k=60N/m, all ten subjects have a lower mean RMSE, and nine of ten subjects have a lower range of RMSE.

V. Conclusion and Future Works

In this paper, a method for variable admittance control in robot-assisted orthopedic surgery was proposed. Instead of modifying virtual damping or mass in previous works, a mean point of robot end effector trajectory in the past T period was used as reference point, and connected with effector by a virtual spring. The performance of the proposed controller was tested by conducting a cooperative experience where the subjects were asked to finish a reaching task by using a Mini-robot. The boundary control ability of subjects was evaluated by using the straightness of trajectory's endpoints. The taken results proved that the proposed method has a lower error in straightness, which means a better performance in human-robot collaboration stability. Nine of all ten subjects consider that the proposed variable admittance controller is better than the traditional admittance controller.

In the near future, the proposed method will be applied for real orthopedic surgery. And further research will focus on adjusting the time period and virtual spring stiffness during the collaboration tasks to make the proposed controller better adapt to the habits of different people.

References

[1] P. Subramanian, T. W. Wainwright, S. Bahadori, and R. G. Middleton, "A review of the evolution of robotic-assisted total hip arthroplasty," HIP Int., vol. 29, no. 3, pp. 232–238, May 2019.

[2] A. Calanca, R. Muradore, and P. Fiorini, "A review of algorithms for compliant control of stiff and fixed-compliance robots," IEEE/ASME Trans. Mechatronics, vol. 21, no. 2, pp. 613–624, 2016.

[3] S. Kuang et al., "A novel passive/active hybrid robot for orthopaedic trauma surgery," Int. J. Med. Robot. Comput. Assist. Surg., vol. 8, no. 4, pp. 458–467, Dec. 2012.

[4] M. L. Swank, M. Alkire, M. Conditt, and J. H. Lonner, "Technology and cost-effectiveness in knee arthroplasty: computer navigation and robotics," Am. J. Orthop., vol. 38, no. 2 Suppl, p. 32, 2009.

[5] D. L. Riddle, W. A. Jiranek, and F. J. Mcglynn, "Yearly Incidence of Unicompartmental Knee Arthroplasty in the United States," J. Arthroplasty, vol. 23, no. 3, pp. 408 – 412, 2008.

[6] Z. Min, H. Ren, and M. Q.-. Meng, "Statistical Model of Total Target Registrati are all current research hotspots.on Error in Image-Guided Surgery," IEEE Trans. Autom. Sci. Eng., pp. 1–15, 2019.

[7] Z. Min, L. Liu, and M. Q.-H. Meng, "Generalized Non-rigid Point Set Registration with Hybrid Mixture Models Considering Anisotropic Positional Uncertainties," in Medical Image Computing and Computer Assisted Intervention -- MICCAI 2019, 2019, pp. 547–555.

[8] N. Hogan, "Impedance Control: An Approach to Manipulation: Part I—Theory," J. Dyn. Syst. Meas. Control, vol. 107, no. 1, p. 1, 1985.

[9] T. Tsumugiwa, R. Yokogawa, and K. Hara, "Variable impedance control with regard to working process for man-machine cooperation-work system," pp. 1564–1569, 2002.

[10] A. Lecours, B. Mayer-St-Onge, and C. Gosselin, "Variable admittance control of a four-degree-of-freedom intelligent assist device," in 2012 IEEE International Conference on Robotics and Automation, 2012, pp. 3903–3908.

[11] H.-Y. Li, T. Nuradha, S. A. Xavier, and U.-X. Tan, "Towards A Compliant and Accurate Cooperative Micromanipulator using Variable Admittance Control," in 2018 3rd International Conference on Advanced Robotics and Mechatronics (ICARM), 2018, pp. 230–235.

[12] A.-N. Sharkawy, P. N. Koustournpardis, and N. Aspragathos, "Variable Admittance Control for Human-Robot Collaboration based on Online Neural Network Training," in 2018 IEEE/RSJ International Conference on Intelligent Robots and Systems (IROS), 2018, pp. 1334–1339.

[13] F. Dimeas and N. Aspragathos, “Reinforcement learning of variable admittance control for human-robot co-manipulation,” in 2015 IEEE/RSJ International Conference on Intelligent Robots and Systems (IROS), 2015, pp. 1011–1016.

[14] F. Dimeas and N. Aspragathos, “Fuzzy learning variable admittance control for human-robot cooperation,” in 2014 IEEE/RSJ International Conference on Intelligent Robots and Systems, 2014, pp. 4770–4775.

[15] Z. Du, W. Wang, Z. Yan, W. Dong, and W. Wang, “Variable Admittance Control Based on Fuzzy Reinforcement Learning for Minimally Invasive Surgery Manipulator,” Sensors, vol. 17, no. 4, p. 844, Apr. 2017.

[16] S. Grafakos, F. Dimeas, and N. Aspragathos, “Variable admittance control in pHRI using EMG-based arm muscles co-activation,” in 2016 IEEE International Conference on Systems, Man, and Cybernetics (SMC), 2016, pp. 001900–001905.

[17] P. Gomes, “Surgical robotics: Reviewing the past, analysing the present, imagining the future,” Robot. Comput. Integr. Manuf., vol. 27, no. 2, pp. 261–266, Apr. 2011.

[18] J. Rahman, K. Al-Tawil, and W. S. Khan, “Use of Robotic-Assisted Surgery in Orthopedics,” in General Principles of Orthopedics and Trauma, Cham: Springer International Publishing, 2019, pp. 629–637.

[19] R. Tarwala and L. D. Dorr, “Robotic assisted total hip arthroplasty using the MAKO platform,” Curr. Rev. Musculoskelet. Med., vol. 4, no. 3, pp. 151–156, Sep. 2011.

[20] P. Song, Y. Yu, and X. Zhang, “Impedance Control of Robots: An Overview,” in 2017 2nd International Conference on Cybernetics, Robotics and Control (CRC), 2017, pp. 51–55.

[21] H. Wang, J. Liu, and Y. Zhang, “New Results on Eigenvalue Distribution and Controller Design for Time Delay Systems,” IEEE Trans. Automat. Contr., vol. 62, no. 6, pp. 2886–2901, Jun. 2017.